

Absolute Electrical Property Imaging Using High Resolution Inductive, Magnetoresistive and Capacitive Sensor Arrays for Materials Characterization

Neil Goldfine, Andrew Washabaugh, Vladimir Zilberstein, Darrell Schlicker, Ian Shay,
David Grundy, Mark Windoloski

JENTEK Sensors, Inc. 110-1 Clematis Avenue, Waltham, MA 02453-7013
Tel: 781-642-9666; Fax: 781-642-7525, email: jentek@shore.net

ABSTRACT

Recent advances in magnetic and electric field sensor arrays provide new capabilities for absolute imaging of electrical conductivity, magnetic permeability and dielectric permittivity. Arrays of inductive or magnetoresistive sensing elements are used with magnetic field drives while arrays of capacitive sensing elements are used with electric field drives. Specific inspection examples include magnetic permeability measurements of applied and residual stress in steels, magnetic permeability measurement of precrack fatigue damage in steels, electrical conductivity measurements in a furnace for heat treatment quality control, multiple frequency electrical conductivity measurements for coating age degradation characterization, imaging of hidden damage (e.g., fatigue and corrosion), and complex permittivity monitoring for curing of epoxies and adhesives. This paper reviews shaped field magnetometer and dielectrometer measurement methods and provides a description of inversion methods for property estimation using physical models.

INTRODUCTION

Shaped field sensors and sensor arrays use novel drive winding or electrode patterns to impose an electromagnetic field on a test material that can be accurately modeled. For low-frequency excitations, where the fields can be considered quasistatic, a magnetic field is used by inductive sensors for conducting and magnetic materials while an electric field is used by capacitive sensors for insulating or weakly conducting dielectric materials. The ability to model the response accurately permits absolute property measurements of the test article with minimal calibration requirements. In many cases, a calibration in air can be performed, where measuring the response in air, away from any other media can correct for variations in cable capacitance, unmodeled parasitic coupling and drift in instrumentation. Practically, this means that extensive, and often expensive, calibration and training sets that match the geometry and material property ranges of the test articles are not required to ensure that the sensor responds predictably over the material property variations of interest. This is possible since there is little sensor-to-sensor variability, compared to conventional sensor designs, as the sensors can be manufactured using microfabrication techniques so that the sensors are highly repeatable and reproducible. The sensors can also be fabricated onto thin, flexible substrates. These attributes make these sensors well-suited for the nondestructive evaluation of materials, including the imaging of material properties over wide areas using sensor arrays. One such example of a shaped-field inductive eddy current sensor designed specifically for the characterization of material properties in the near-surface region is the Meandering Winding Magnetometer (MWM[®]) [Melcher, 1991, Goldfine, 1995]. This paper provides an overview of shaped-field inductive and capacitive sensor designs and describes their use in several applications.

SHAPED FIELD SENSORS

Shaped field sensors and sensor arrays use drive winding or electrode patterns that provides a desired spatial distribution for the imposed magnetic or electric field. For inductive or GMR-based sensors, a drive or primary winding shapes the magnetic field. For capacitive sensors, drive electrodes shape the electric field.

Figure 1 provides examples of MWM and MWM-Array sensors. A drive winding, with linear drive segments, is excited with a current at a prescribed frequency, typically between 100 Hz and 40 MHz, for inspection of conducting and/or magnetic materials. The drive current produces a time varying magnetic field that induces eddy currents in conducting test materials that follow the drive winding geometry. Inductive sensing coils sense the absolute variations in the magnetic field due to the proximity of the test material and the presence of local defects or geometric features that alter the flow of the eddy currents. The use of relatively small sensing elements, e.g., down to 1 mm by 1 mm squares, permits high resolution imaging of the properties. High resolution imaging is critical for detection of small cracks, while absolute imaging is critical to correct robustly for lift-off variations. Sensing elements other than coils, such as giant magnetoresistive (GMR) sensors, can also be used to sense the changes in the magnetic field directly, which is particularly useful at low frequencies as a GMR sensor responds directly to the magnetic field while an inductive coil responds to the time rate of change of the magnetic field.

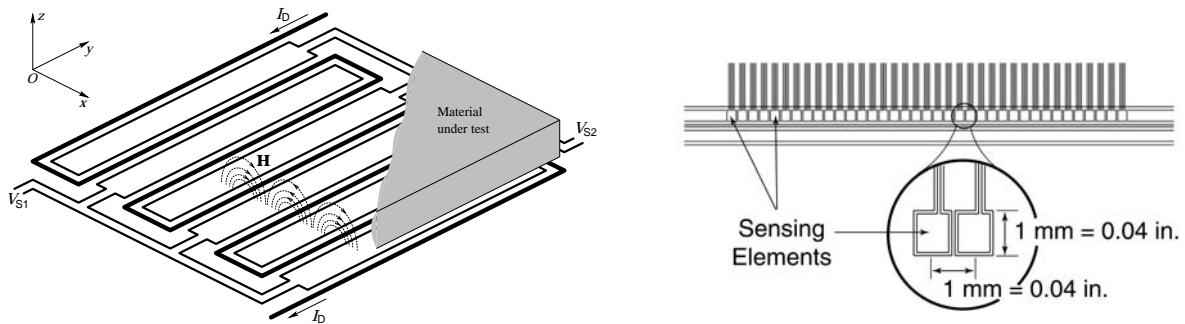


Figure 1. (left) Schematic of a periodic field MWM for absolute property measurements; and (right) schematic of a single wavelength MWM-Array with 1 mm x 1 mm square sensing elements for property imaging.

The basic structure for quantitative single sided dielectrometry measurements is the interdigitated electrode dielectrometer (IDEDTM) sensor shown in Figure 2 [Zaretsky, 1988]. One set of electrode fingers is driven at a voltage at a prescribed frequency, typically between 0.005 Hz and 10 MHz, for inspection of insulating or weakly conducting dielectric materials. The drive voltage produces an electric field that passes through the test material and couples to a second set of electrode fingers that float to a sense voltage or are virtually grounded for a sense current. This sensor can be thought of as two parallel plate electrodes laid flat to lie in a single plane to cause a fringing electric field region that penetrates into the unknown dielectric. The depth of sensitivity is approximately 1/3 of the spatial periodicity of the electrodes or fundamental spatial wavelength λ , so that small wavelength sensors will primarily respond to changes of material properties near the sensor-material interface, while larger wavelength sensors respond to changes farther from the sensor interface. Thus multiple wavelength sensors can be used to measure spatial profiles of dielectric properties or the air gap (lift-off) between the sensor and test material, making them well suited to single-sided noncontact dielectric measurements [Melcher, 1989]. Arrays of sensing elements are

created by segmenting the sense electrode into individual electrodes along the length of a "finger." Alternatively, multiple wavelength sensor arrays can be formed by meandering additional sense electrodes between the drive and sense electrodes.

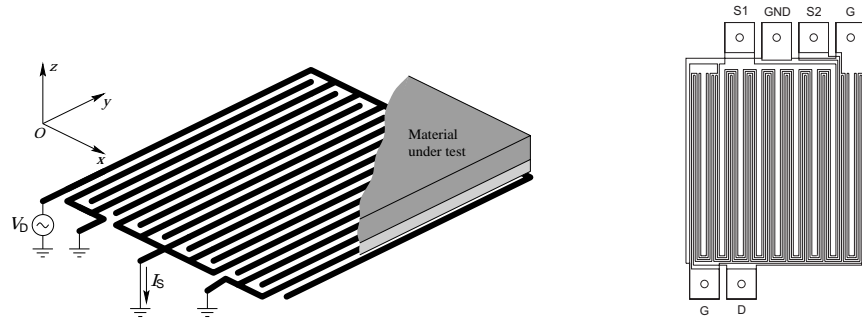


Figure 2. (left) Schematic of a periodic field IDED for absolute property measurements; (right) schematic for a two-wavelength co-located interdigitated electrode sensor.

MEASUREMENT GRID INVERSION METHODS

A convenient method for converting the measurement data into material property estimates is to use grid measurement methods, which use a database of sensor responses to map the measured signals into the physical properties of interest. [Goldfine, 1997]. The database is generated, prior to data acquisition, using a physical model of the sensor response to various material properties and layer thicknesses. Two-dimensional subsets of the database can be visualized as a measurement grid that relates two measured parameters (such as the magnitude and phase of the transimpedance between the MWM drive and sense windings, the IDED transadmittance magnitude and phase measured at the electrode terminals, or the magnitude of two IDED sensors with different spatial wavelengths) to two unknown parameters of interest, such as the permittivity and conductivity of a dielectric layer or permittivity and lift-off. These grids are then used to provide real time conversion of the measurement data into properties of interest. This algorithm for quantitative property determination is readily implemented in the data acquisition instrumentation software. The alternative, conventional, technique for solving the inverse problem is to use a method that iteratively applies a forward model that computes the sensor response from the physical properties of the material and the sensor geometry. This technique is relatively slow and is not guaranteed to converge to a physical solution.

REPRESENTATIVE APPLICATIONS

Stress Measurements – Directional magnetic permeability measurements by MWM sensors and MWM-Arrays allow estimation of stresses by taking advantage of the magnetostriction effect [Zilberstein, 2002]. For steels, at magnetic fields typical of those used for the MWM, the magnetostriction coefficient generally is positive. This means that the magnetic permeability for steels would increase with tensile stress. Thus, once a correlation between stress and MWM measured magnetic permeability is established, stresses can be estimated as long as baseline information is available. MWM permeability measurements on 300M high-strength steel specimens under fully reversed bending loading provide one such correlation with stress. The tests were performed on flat shot peened specimens installed in a bending fixture. Permeability measurements were performed with a single-sensing element MWM sensor placed on the specimen

with the longer segments of the drive winding perpendicular to the bending stress direction so that the permeability in the specimen longitudinal direction is measured. Figure 3 shows the permeability variation with applied bending stress at measurement frequencies of 40 kHz, 100 kHz, and 1 MHz. The differences in measured permeability at the high and low frequencies are attributed primarily to an interaction between compressive stresses from shot peening and applied stresses. The data illustrate the sensitivity of the MWM measurements for applied stress measurements in high strength steels over a wide range of stresses. The results clearly show the sensitivity of the MWM measurements to stress changes and reasonably small hysteresis, particularly in the compressive stress range.

MWM-Arrays provide a capability to perform bi-directional magnetic permeability measurements in a scanning mode. This capability permits determination of the residual stress distribution in parts fabricated from carbon and low-alloy steels. As an example, an MWM-Array was scanned across and along the gage section of a specimen broken in a tensile test. The image of MWM measured permeability for measurement frequency of 158 kHz indicates a high residual stress region near the fracture. Comparison of this image with an image obtained at 1 MHz indicates that the zone of lower permeability is caused by compressive residual stresses and not by a surface condition.

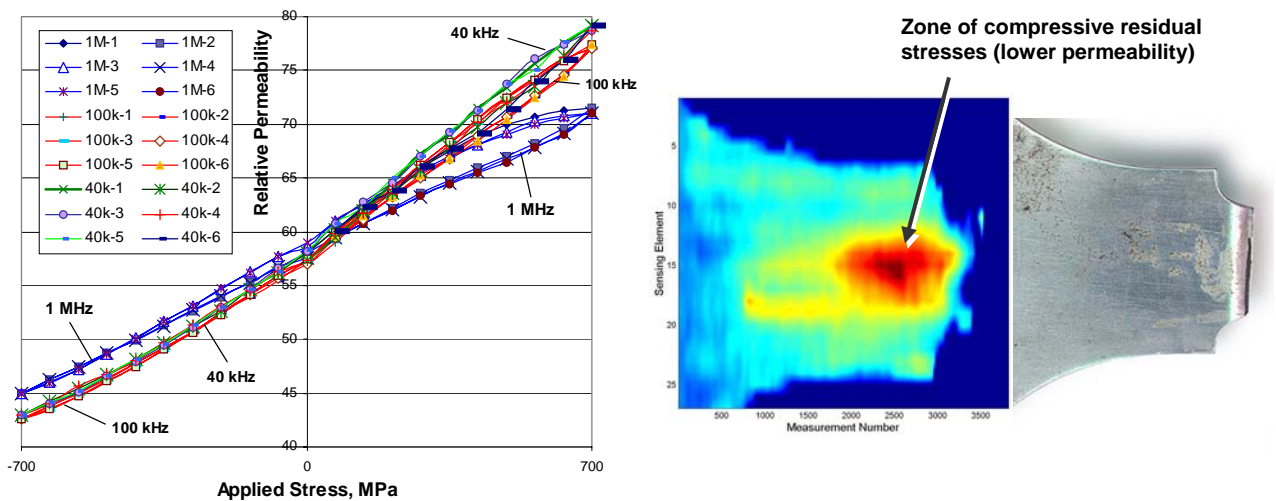


Figure 3. (left) MWM measured permeability vs. bending stress at stresses from -700 MPa to $+700$ MPa. (right) MWM-Array generated normalized 158 kHz permeability image and photograph of one half of a double-notched, low-alloy 4340 steel specimen, which failed in a tensile test. For this image, the primary winding of the MWM-Array was oriented perpendicular to the loading axis.

Detection of Precrack Fatigue Damage in Steels – MWM Sensors have been used to detect fatigue damage in steels prior to formation of detectable cracks. Figure 4 illustrates this capability for originally annealed austenitic stainless steel, which forms martensite of deformation during cyclic loading. Formation of this ferromagnetic phase is captured by MWM permeability measurements. Recent fatigue tests of 4340 steel specimens with an MWM-Array mounted in the gage section revealed the capability to detect precrack fatigue damage early in the fatigue life. Figure 5 shows MWM measured permeability changes (using a permanently mounted MWM-Array) during such a fatigue test, indicating early fatigue damage detection.

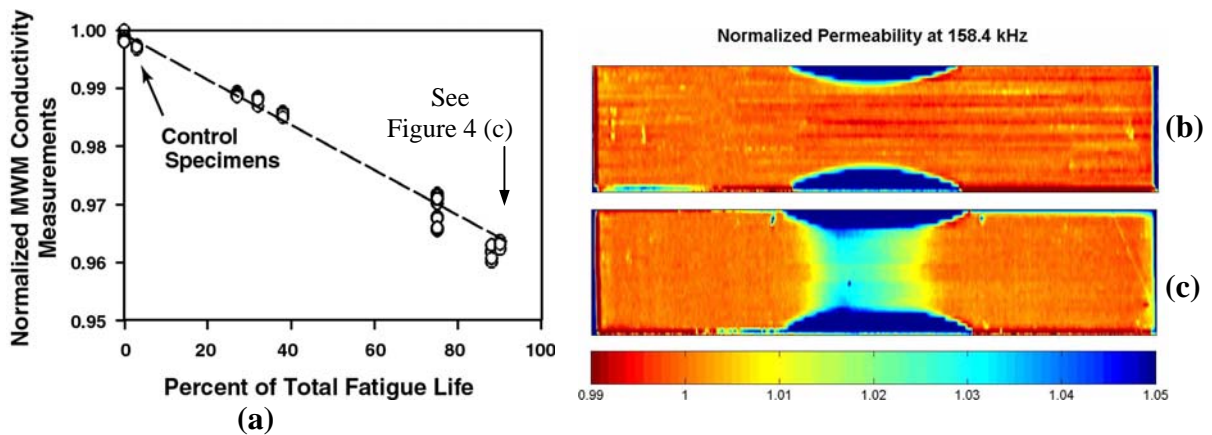


Figure 4. (a) Effective conductivity changes as a function of percent of fatigue life for Type 304 stainless steel specimens. Each specimen was tested to a fraction of total life. The total life was determined as a mean number of cycles to failure with a separate set of specimens from the same lot as the specimens tested to a fraction of life and tested under the same test conditions. (b) Magnetic permeability image for a control annealed specimen that has not been subject to fatigue testing. (c) Magnetic permeability image for the specimen tested to 88% of fatigue life. The images in (b) and (c) were generated with an MWM-Array.

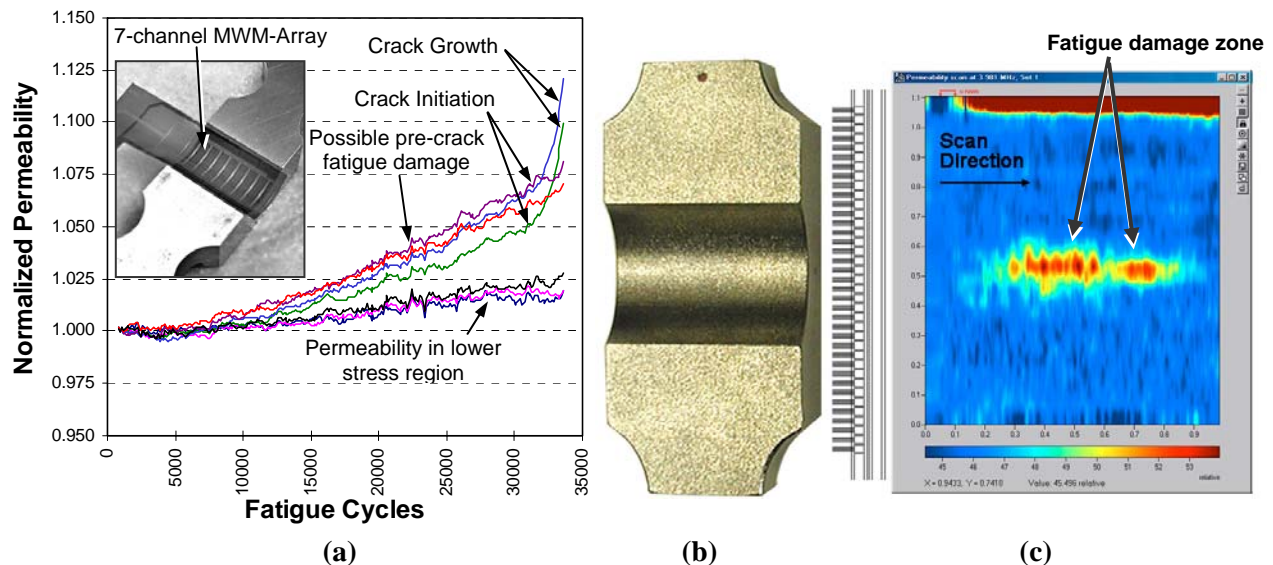


Figure 5. (a) Normalized permeability vs. fatigue cycles (permeability measured with a permanently mounted MWM-Array) for a shot peened 4340 specimen shown in (b). Initial permeability increase starting at about 7000-8000 cycles might be related to precrack fatigue damage, while a sharp increase starting at about 31,000 cycles is caused most likely by crack initiation and growth. (c) An image of the fatigue damage zone obtained by a scanning MWM-Array.

Heat Treatment Monitoring – A single-channel MWM sensor constructed of copper conductors on a Kapton™ substrate using widespread and low-cost microfabrication techniques is traditionally operated at ambient temperatures. Recently, modifications to the standard MWM sensor configuration allowed lift-off and conductivity measurements of an aluminum 2024 coupon to be made during various heat treatments at temperatures up to 270°C. Shown in Figure 6 are plots of conductivity versus temperature for the aluminum 2024 coupon as the original T3 condition was overaged and then reheated. Following a solution anneal to produce the T42 condition, the coupon was again heated to monitor conductivity changes as the T62, T72 and overaged conditions were achieved.

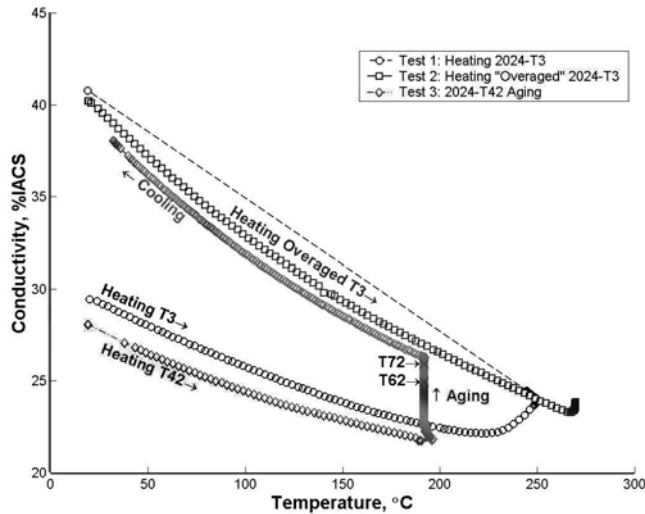


Figure 6. MWM measured conductivity changes for Al 2024 at temperatures up to 270°C.

Hidden Corrosion Imaging – Figure 7 provides a quantitative thickness image of a C-130 flight deck chine plate, illustrating the imaging of hidden corrosion. This image was taken from the exposed side of the plate using a 94 mm wide MWM-Array in 3 passes with a manual scanning cart and a single rolling position encoder. The scan speed was 75 mm/s, so that the creation of the image took only a few seconds per scan. This illustrates the potential to image hidden geometric features and measure wall thickness in components [Goldfine, 2002], as well as the ability to manually scan wide areas and build high resolution images without expensive scanners.

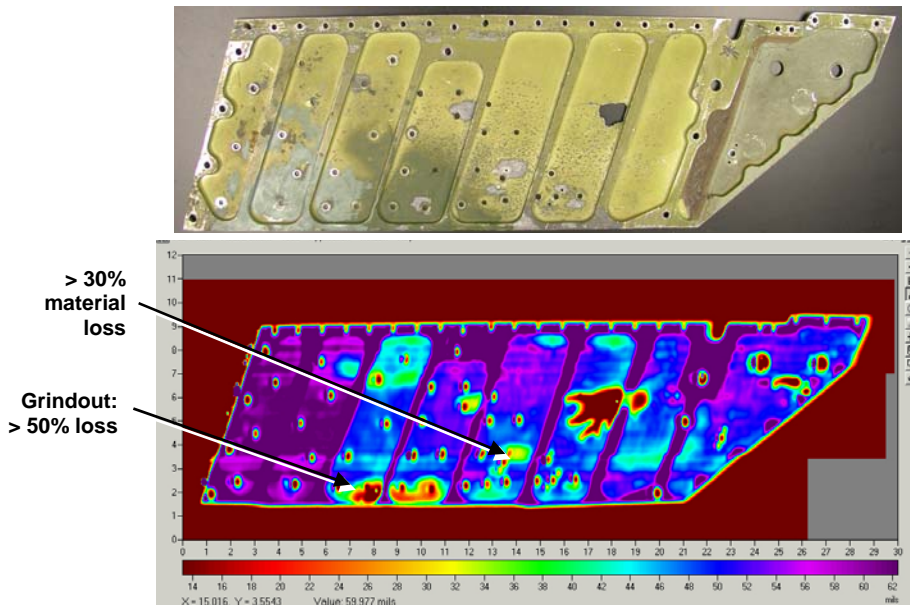


Figure 7. Photograph (top) and MWM-Array generated thickness image (bottom) of C-130 flight deck chine plate. The MWM image reveals hidden corrosion and geometry created by scanning on the accessible side (opposite from the normally inaccessible side shown in the photograph).

Coating Characterization – Multiple frequency measurements provide a method for determining more than two parameters associated with the material property measurement. For example, a grid

based algorithm has been developed for conducting coating evaluation, such as production turbine blade coatings, to determine the coating thickness, the coating conductivity, and the sensor lift-off assuming that the conducting substrate properties are known. A multiple frequency approach has also been used to characterize aged coatings, which can have several layers of varying properties. As part of an EPRI round robin study, coating degradation was assessed through measurement of the remaining beta zone layer thickness for a PWA286 coating on a superalloy substrate [Goldfine, 2001]. Results are shown in Figure 8. The flat conductivity response shows the baseline response of the non-aged substrate, the uppermost curve corresponds to the as-coated sample, and the aged samples show a progression of decreasing effective conductivity across the frequency range with increasing degradation. The MWM measurement results were analyzed using an estimation algorithm based on a model for the sensor response to obtain the various layer thicknesses.

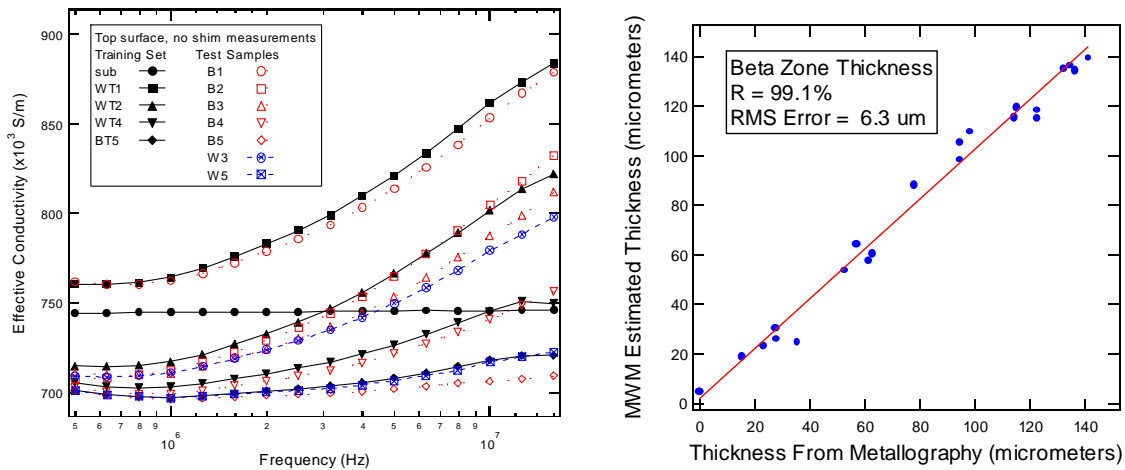


Figure 8. (Left) Comparison of the MWM multifrequency effective conductivity measurements for training set and blind test samples; (right) MWM measured beta-phase layer thickness versus reported beta-phase layer thickness for blind test set.

Epoxy Cure Monitoring – Figure 9 shows an example measurement grid for monitoring the cure state of a thick layer of epoxy placed over an IDED sensor. The thickness of the epoxy layer (Δ_c) is large compared to the sensor wavelength so that the epoxy can be modeled as an “infinitely” thick layer. To permit reuse of the sensor, the epoxy is placed on top of a disposable polymer layer. As the epoxy cures, the magnitude and phase of the sensor transmittance change as illustrated on the measurement grid. Interpolation of these data points on the grid then provides the transient measurements of the permittivity and conductivity for the curing epoxy. The time and value of the peak in the permittivity and conductivity are dependent upon the chemistry of the epoxy and reflect the cure state of the material. Figure 9 shows, for these chemistries, that the nominal cure time is reflected in the time transient variation in the conductivity, rather than the permittivity. A similar measurement might be made in a noncontact mode if two IDED spatial wavelengths are included to correct for lift-off variations [Schlicker, 2002].

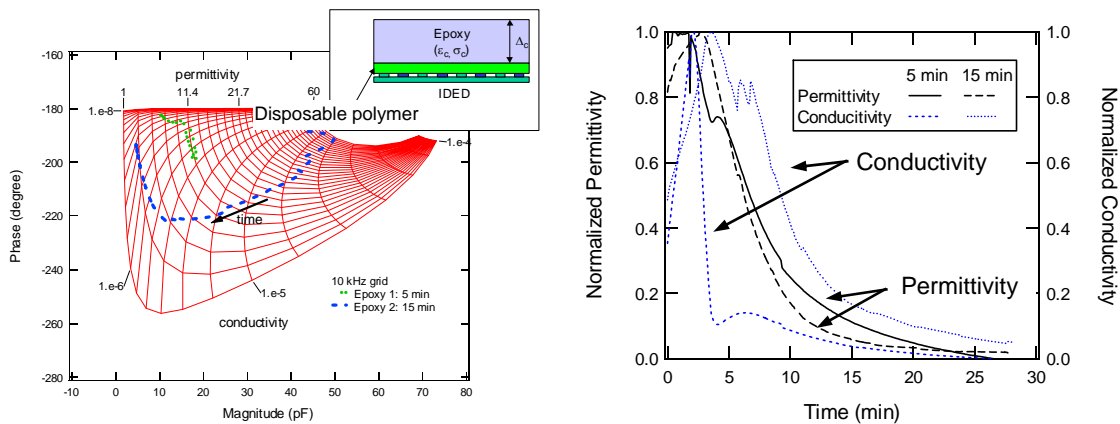


Figure 9. (left) Measurement grid with data for epoxy cure measurements. (right) Effective property estimates normalized by the peak value.

CONCLUDING REMARKS

This paper reviewed some of the nondestructive materials characterization and measurement capabilities of shaped field magnetic and electric field sensors. The magnetic field sensors, which use either inductive coils or GMR sensors as sense elements, can be used to characterize conducting and magnetic materials. The electric field sensors use capacitive coupling to characterize insulating or weakly conducting dielectric materials. Both technologies have demonstrated significant capabilities for a wide range of inspection and materials characterization applications, including precrack fatigue damage detection, hidden corrosion imaging for metals, and cure state monitoring for epoxies.

REFERENCES

- Melcher, J.R., (1991), "Apparatus and Methods for Measuring Permeability and Conductivity in Materials Using Multiple Wavelength Interrogations," US Patent No. 5,015,951.
- Goldfine, N.J., and Melcher, J.R. (1995), "Magnetometer Having Periodic Winding Structure and Material Property Estimator," U.S. Patent No. 5,453,689.
- Melcher, J.R., et. al., (1989), "Apparatus and Methods for Measuring Permittivity in Materials", U.S. Patent No. 4,814,690.
- Goldfine, N.J., et. al., (1997), "Apparatus and Methods for Obtaining Increased Sensitivity, Selectivity, and Dynamic Range in Property Measurements using Magnetometers," U.S. Patent No. 5,629,621.
- Goldfine, N., D. Grundy, V. Zilberstein, D. Schlicker, I. Shay, A. Washabaugh, M. Windoloski, M. Fisher, K. LaCivita, V. Champagne (2002), "Corrosion Detection and Prioritization Using Scanning and Permanently Mounted MWM Eddy-Current Arrays," Tri-Service Corrosion Conference, San Antonio, TX.
- Goldfine, N., et. al., (2001), "Conformable Eddy-Current Sensors and Arrays for Fleet-wide Gas Turbine Component Quality Assessment," ASME Turbo Expo Land, Sea & Air, New Orleans, LA.
- Schlicker, D., I. Shay, A. Washabaugh, N. Goldfine, 2002, "Capacitive Sensing Dielectrometers for Noncontact Characterization of Adhesives and Epoxies," SPE ANTEC Conf., San Francisco, CA.
- Zaretsky, M.C., et. al., (1988), "Continuum Properties from Interdigital Electrode Dielectrometry," IEEE Trans. on Elec. Ins., Vol. 23, No.6, Dec. 1988, pp. 897-917.
- Zilberstein, V., et. al., (2002), "Residual and Applied Stress Estimation from Directional Magnetic Permeability Measurements with MWM Sensors." Accepted for publication to ASME Journal of Pressure Vessel Technology, August 2002 issue.